 https://doi.org/10.3311/PPme.41586

Periodica Polytechnica Mechanical Engineering, 69(3), pp. 278–285, 2025

Production and Testing of Syntactic Metal Foams Reinforced with Aluminium-silicon Partially Infiltrated Carbon Fibre Bundles

Benedek Szovák[1,2*], Alexandra Kemény[1,2], Imre Norbert Orbulov[1,2]

[1] Department of Materials Science and Engineering, Faculty of Mechanical Engineering, Budapest University of Technology and Economics, Műegyetem rkp. 3., H-1111 Budapest, Hungary
[2] MTA-BME Lendület "Momentum" High-performance Composite Metal Foams Research Group, Műegyetem rkp. 3., H-1111 Budapest, Hungary
[*] Corresponding author, e-mail: szovak.benedek@edu.bme.hu

Received: 12 July 2025, Accepted: 07 August 2025, Published online: 25 August 2025

Abstract

Syntactic metal foams are porous materials with outstanding specific mechanical properties, such as high specific energy absorption and specific load-bearing capacity. However, due to the cellular structure, they are not suited for handling tensile loads. This study aims to create a composite structure in which carbon fibre bundles are embedded along the load direction in syntactic metal foams. The samples were produced by pressure infiltration of the fillers and the pre-infiltrated carbon fibre bundles. Tensile tests show that the fibre bundles increase the tensile load-bearing capacity of the specimens. The reference samples withstood 0.69 ± 0.07 kN tensile force. The reinforcement increased the density of the metal foam by 20% (from 1.21 ± 0.01 g·cm^{-3} to 1.52 ± 0.01 g·cm^{-3}), while increasing the tensile load-bearing capacity to 1.80 ± 0.15 kN, an approximate increase of 260%, and 1.27 ± 0.10 kN an approximate increase of 180% in the case of 6 and 4 reinforcing carbon fibre bundles, respectively. The relationship between the load-bearing capacity (peak force) and the number of reinforcing carbon fibre bundles can be exactly described by a second-order polynomial function and can also be estimated by a simpler linear relationship.

Keywords

metal foams, syntactic metal foams, fibre reinforcement

1 Introduction

Metal foams are cellular materials with a metal matrix in which there are gas-filled pores. Their density is low compared to their bulk base material [1]. Different types of metal foams can be half to one-third as dense as the bulk form of the matrix material. The different metallic foam types can be categorised as open-cell foams with interconnected porosity [2–6], or closed-cell foams [7–10] where the individual cells are completely separated. Metal matrix syntactic foams (MMSFs) are a subgroup of closed-cell metal foams in which the porosity is formed by introducing hollow filler material to the metal matrix [11–16]. MMSFs have good mechanical properties, such as a high energy absorption capacity during compression, due to the strength and crush behaviour of the fillers. However, they cannot effectively handle tensile load due to (i) inner porosities that serve as starting points for cracks and (ii) the complex load of the matrix struts and layers between the fillers [16, 17].

MMSFs can be considered as composite materials because two materials are combined within them, [18–22]. Composite structures can be utilised to negate the disadvantages of two materials by combining them in a structure [23, 24] and to emphasise the advantages of the constituents (low-density matrix and high-strength bundles). Reinforcement material particles, which can handle the required load, are embedded in a matrix material that holds the particles together, protects them from environmental damage, and transmits the load to them. The reinforcement particles can be in the form of grains, fibres, fibre bundles, or quilts [25–27]. Different forms provide different advantages. Grains, short fibres, and quilts provide reinforcement in all directions, while fibres and fibre bundles provide reinforcement in only the direction of the fibres but with a greater effect. By the proper alignment of the bundles, the load-bearing capacity can be enhanced

Cite this article as: Szovák, B., Kemény, A., Orbulov, I. N. "Production and Testing of Syntactic Metal Foams Reinforced with Aluminium-silicon Partially Infiltrated Carbon Fibre Bundles", Periodica Polytechnica Mechanical Engineering, 69(3), pp. 278–285, 2025. https://doi.org/10.3311/PPme.41586

significantly (even doubled). The most important challenge here is the alignment of the bundles and fixing them in the proper position during the sample production.

Carbon fibres and carbon nanotubes are ideal for lightweight reinforcement because they are strong yet low in density [28–30]. However, short fibres and nanotubes tend to form clusters, which block homogeneous distribution and significantly hinder the liquid state production methods because of the hard wetting conditions (large contact angles, high surface tension and oxidation of the molten matrix material). MMSFs are particularly susceptible to this effect, and due to that the fibres need to be distributed between the filler particles. However, the use of short fibres is a viable solution to increase the pore size during gas injection foaming process [31].

The aim of this study is to create a composite structure where carbon fibre bundles are placed unidirectionally inside MMSFs filled with expanded glass particles. The main goal through this method is to create a composite structure in which the fibre bundles can effectively handle tensile load and improve the tensile mechanical properties of the MMSFs without increasing (at least significantly) the density of the structure – further improving the specific properties.

2 Materials and methods

2.1 Materials and their characterisation methods

Al99.5 aluminium was used as the matrix material owing to its high ductility, low density, relatively low price and availability. The chemical composition of the matrix was measured with a WAS PMI-MASTER SORT spectrometer (Worldwide Analytical Systems AG, Uedem, Germany). The chemical composition was found to be 99.5 wt% Al, containing 0.335 wt% Fe and a negligible amount of common trace elements for Al alloys (Sn, Si, Ni, Zn, Cu, Cr, Mn, Mg and Ti).

As reinforcement, aluminium-silicon (AlSi12) alloy pre-infiltrated carbon fibre bundles, with a diameter of Ø1.00±0.05 mm were applied. The bundles are shown in Fig. 1(a). The bundles were manufactured in the laboratory in the framework of a previous research [32]. The partially infiltrated composite wires were made of Al99.5 matrix and Thornel P4K type carbon fibres by liquid state continuous pressure infiltration, or so-called Blücher's method. The matrix was overheated to 700 °C, and the applied pressure difference to infiltrate the tow was 1 MPa. The pulling velocity was 15 m/min, consequently, the exposure time (the time that the fibres spent in molten metal) was approximately 0.2 s. Further details about the process in general are available in [33–35]. The cross section of the bundle is shown on Fig. 1(b).

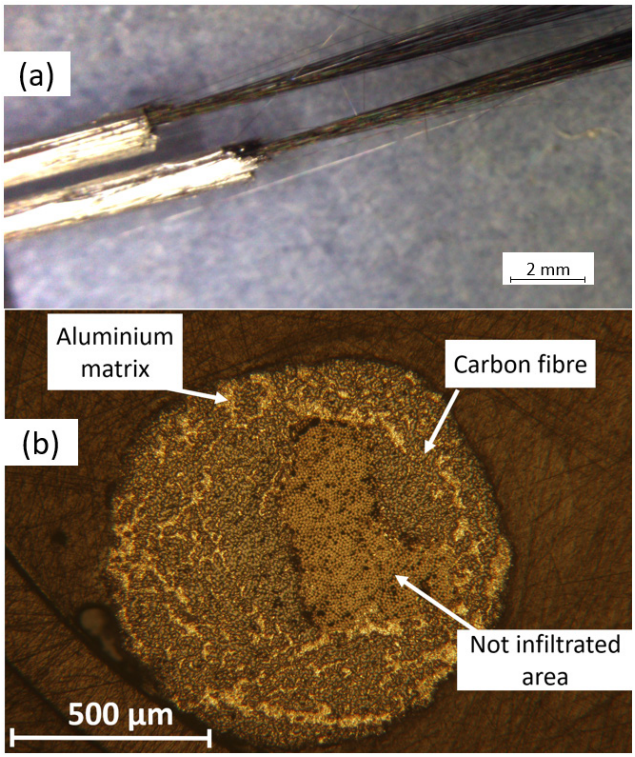

Fig. 1 (a) Partially infiltrated carbon fibre bundles and (b) their structure in the cross section

The image shows that the bundles are only partially infiltrated (creating a special coating) but not completely infiltrated with the AlSi12 alloy. The electron microscopic images of the surface of the bungle are shown in Fig. 2. Fig. 2(a) shows a representative site within the partially infiltrated zone of the carbon fibre bundles, proving complete filling of the small spaces between the individual carbon fibres by the AlSi12 matrix. Fig. 2(b) shows the structure of the partially infiltrated bundles in the coated zone, revealing the close connection of the constituents and the microstructure of the matrix. The chemical composition of the AlSi12 material used to partially infiltrate the carbon bundle was measured with Energy Dispersive Spectrometry (EDS) on a Zeiss EVO MA 10 Scanning Electron Microscope (SEM) (Carl Zeiss AG, Oberkochen, Germany) with an EDAX Octane Elect EDS/EDX detector (Gatan Inc., Pleasanton, United States of America). The chemical composition was found to be 86.100 wt% Al, 12.830 wt% Si and the remaining trace elements.

As filler material, expanded glass from Stikloporas (Stikloporas UAB., Druskiniknkai, Lithuania) with a diameter range of Ø3.02 ± 0.96 mm was chosen owing to

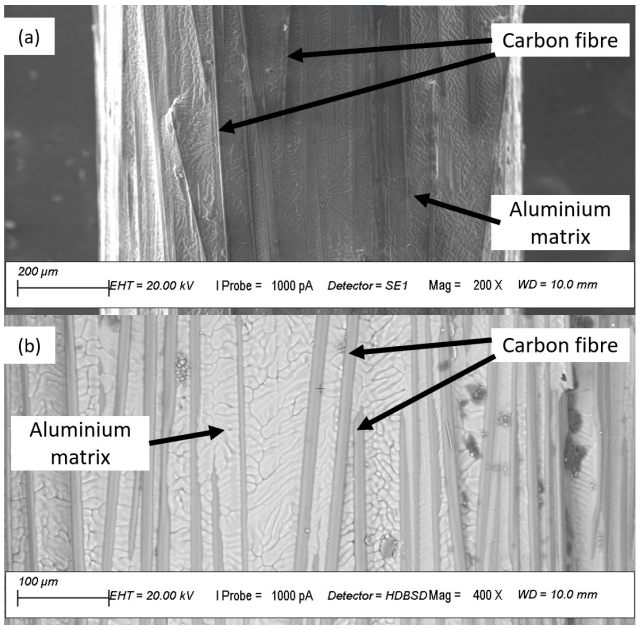

Fig. 2 SEM images of the coating of fibre bundles with different magnifications (a) showing the perfect infiltration and (b) the structure of the bundles

its low density (the particle density is 0.41±0.02 g·cm-3 while the bulk density is 0.23±0.05 g·cm-3), availability, and price. The chemical composition of the fillers was acquired from the manufacturer and it was reported as 71.0-73.0 wt% SiO_2, 13.0-14.0 wt% K_2O + Na_2O, 8.0-10.5 wt% CaO + MgO, 1.5-2.0 wt% Al_2O_3. <0.3 wt% Fe_2O_3 and <0.5 wt% other oxides. The filler material is shown in Fig. 3(a), and its inner porous structure in Fig. 3(b).

2.2 Production of the composite and testing methods

The reinforcement fibre bundles (42 bundles) were placed in an S235JR orienting frame that measured 56 × 56 × 150 mm. The distance of the bundles was set by 1.4307 (X2CrNi18-9) stainless steel meshes with an opening of 2.4 mm at both ends of the orienting frame. A bundle was placed at every second opening. A bundle was placed at every second opening. Then the frame was placed inside an S235JR made mould with outer dimensions of 60 × 60 × 320 mm and a wall thickness of 2 mm. The inner surface of the mould was previously coated with graphite (N 77, Dueci Electronic, Italy) emulsion.

The space between the bundles was evenly filled with filler material particles. The frame was designed to create space alongside the bundles at both ends of the frame, where the filler material cannot flow in. By this, the molten matrix could fill out the space around the bundles to create a solid part for clamping during tensile tests. For reference samples, another mould was filled with the filler material

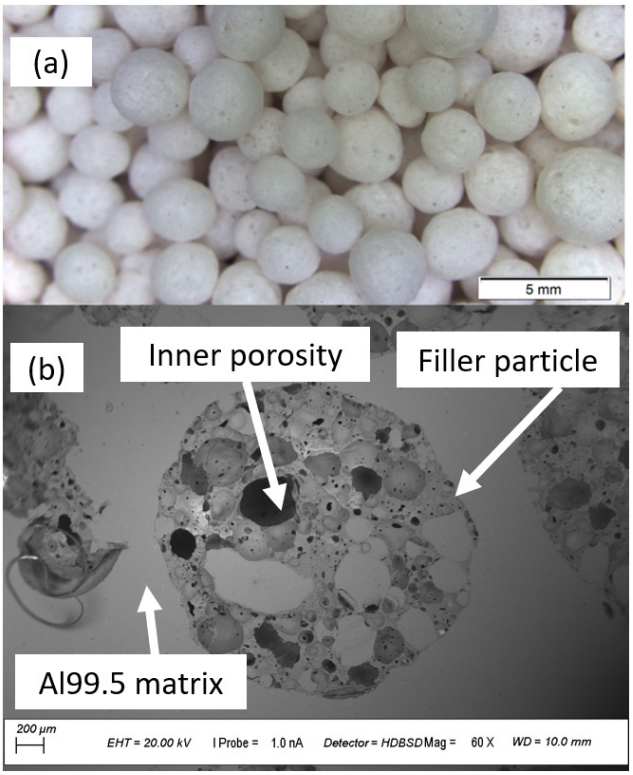

Fig. 3 (a) Expanded glass filler material; and (b) the inner porous structure of the filler material particles

only. A piece of stainless-steel mesh was placed on top to prevent the filler particles from moving up during the infiltration, as their particle density is low.

The compilation was pre-heated to 550 °C in a box furnace (Blue M, Lindberg). The melted matrix was heated up to 750 °C in an induction furnace (B-70 type, Prothermo Hofmann), and was poured into the mould. The infiltration was performed with 99.9% pure argon gas at a pressure of 0.5 MPa. The crucible was cooled in air till it reached room temperature.

Specimens for microscopy and quasi-static tensile tests were prepared with conventional cutting methods. The specimens meant for microscopy were ground by hand with grain sizes from P80 to P4000 and polished with diamond suspension with grain sizes of 3 µm and 1 µm for approximately 30 seconds with each grain size, with a rotation speed of 250 rpm. The polished samples were examined with optical microscopy and SEM. The density of the specimens was calculated from mass and volume measured with a precision scale (with an accuracy of 0.0001 g) and calliper (with an accuracy of 0.01 mm). Energy Dispersive Spectrometry (EDS) was carried out on the reinforcing bundles to determine the composition of the coating.

The tensile test was carried out according to ISO 6892-1:2019 [36] standard. For the test, cylindrical

tensile specimens with a diameter of Ø20 mm and 100 mm gauge length were prepared. The tests were carried out on a TiraTest 2000 universal material testing machine (TIRA GmbH, Schalkau, Germany) with a crosshead speed of 4 mm·s^{-1}. Three specimens were prepared with reinforcement and three specimens without reinforcement for reference. Force and elongation data were drawn from the test in order to examine the maximum force withstood by the specimens.

3 Results and discussion

The samples' placement of reinforcing fibre bundles varied greatly, despite the structure provided by the orienting frame. An image of the structure of the fibre reinforced metal foam is shown in Fig. 4.

Fig. 5 shows the microstructure of the sample in two different magnifications. The images show that the matrix created an adequate bond with the filler particles and the reinforcement. There was negligible amount of unintended gas porosity in the structure and no unwanted segregation on the edge of fibre bundles or filler particles. Fig 5.(b) also shows a thin diffusion zone with minimal amount of silicon diffusion between the AlSi alloy coating and the matrix material.

To further characterise the microstructural features of the composite, line EDS measurements were done. A representative example, intentionally showing a less infiltrated carbon fibre bundle, is shown in Fig. 6. The vicinity of the measurement is presented in Fig. 6(a), with a measurement line starting from the matrix, crossing a partially infiltrated carbon fibre bundle and ending in the matrix again. The corresponding element distribution, considering the most important Al, C, O and Si elements

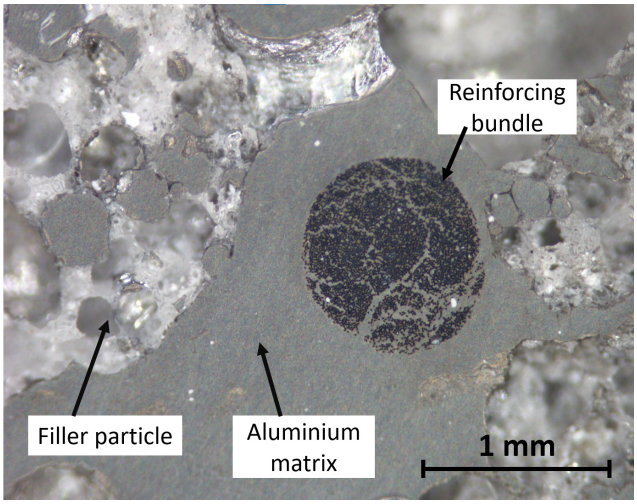

Fig. 4 Microscopic image of the structure of reinforced metal foam, showing the matrix, an individual completely infiltrated reinforcing carbon fibre bundle and the fillers

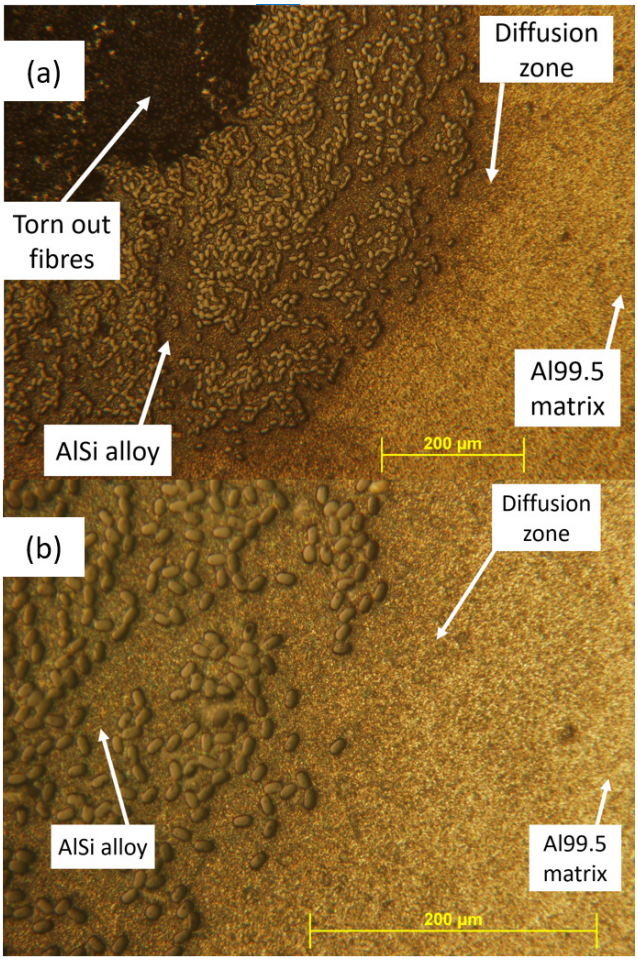

Fig. 5 (a) The microstructure of the fibre bundle reinforced metal foam and (b) a higher-magnification image of the diffusion layer

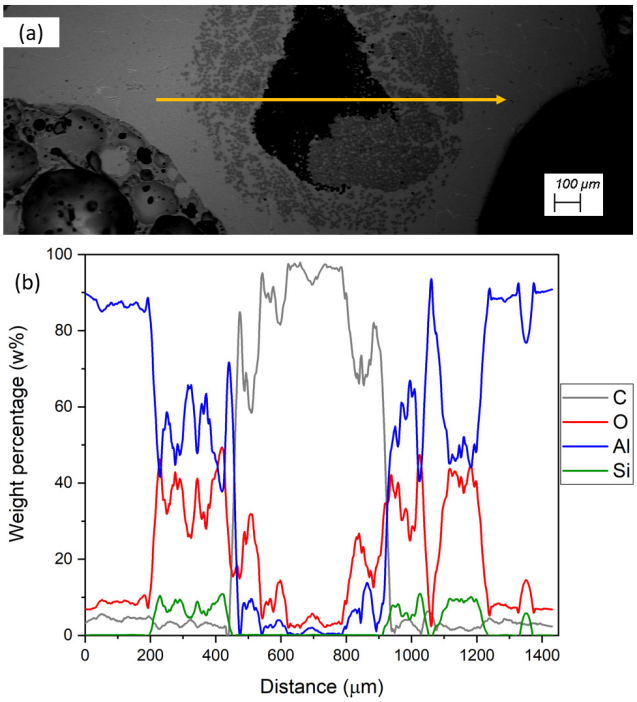

Fig. 6 (a) Direction and placement of the line EDS measurement, and (b) the chemical composition alongside the line

is shown in Fig. 6(b). The low amount of aluminium and silicon between 600 µm and 800 µm indicate that fibres were torn out from the not infiltrated region of the bundles. This phenomenon is shown also in Fig. 5(a).

The cross section of the specimen is shown in Fig. 7. The number of reinforcement bundles was examined after tensile tests on each specimen.

After the structural features, the physical properties were examined. The density of the unreinforced reference samples was 1.21 ± 0.01 g·cm^{-3} while the density of the reinforced samples was 1.52 ± 0.10 g·cm^{-3}. This corresponds to a 20% increment. The explanation of this is that the bundles make the flow of filler material particles more difficult. This led to lower filling percentage around the bundles. The higher deviation in the density of the reinforced samples correlates with the number of reinforcement bundles in the sample.

In order to investigate the load-bearing capacity of the samples, tensile tests were conducted on three samples. After testing, the specimens were cut and polished to enable the number of fibre bundles in a sample to be determined. The numbers varied between 4 and 6. The placement of the bundles is greatly affected by the way the specimens are machined. The force-elongation curves of the tensile tests are shown in Fig. 8.

As shown in the diagram, the specimens' ability to withstand force increased with reinforcement. The reference specimens showed 0.69 ± 0.07 kN load-bearing capacity. Meanwhile, the maximum force withstood by the reinforced specimens was 1.80 ± 0.15 kN (~260% capacity) and 1.27 ± 0.10 kN (~180% capacity) in the case of 6 and 4 reinforcing bundles, respectively. The reinforced samples

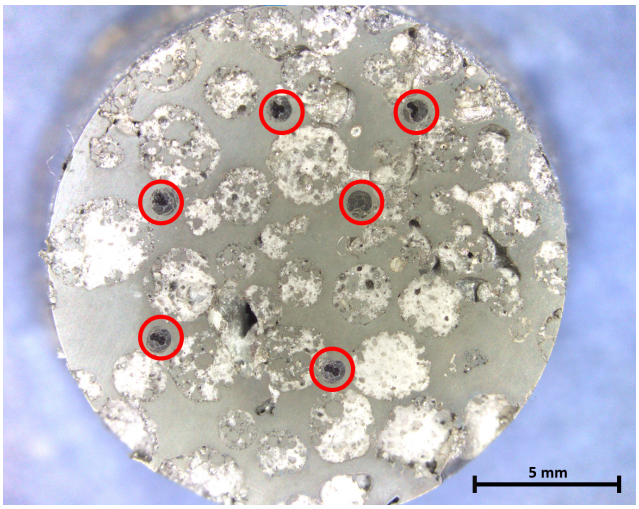

Fig. 7 Macroscopic structure of the specimen in the cross section, with the reinforcement fibre bundles marked

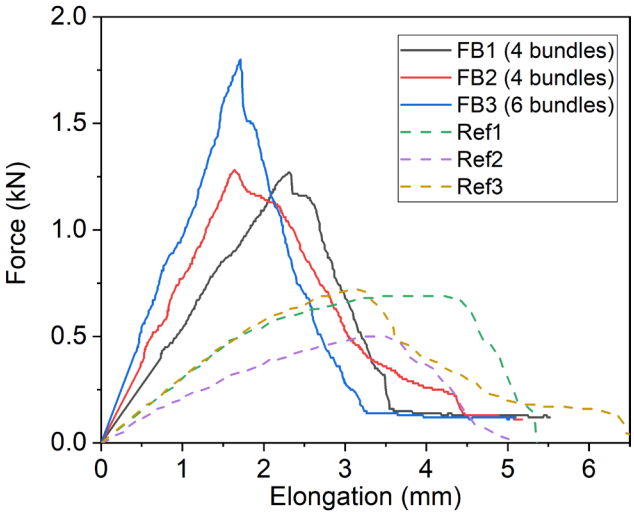

Fig. 8 Force-elongation curves of the tensile tests in the case of (a) reinforced and (b) reference samples

had a more brittle behaviour and reached lower elongation values. The correlation between the load-bearing capacity increment and the number of fibre bundles can be exactly described by a second-order polynomial function (Eq. (1)).

$$F = 0.069 + 0.054N + 0.022N^2\,, \tag{1}$$

where F is the load-bearing capacity, expressed in kN, and N is the number of the reinforcing carbon fibre bundles. The relationship can also be estimated by a simpler linear relationship (Eq. (2)).

$$F = 0.067 + 0.17N \quad (R^2 = 0.975)\,, \tag{2}$$

where F and N have the same meaning as in the case of Eq. (1). Both relationships have been visualised in Fig. 9.

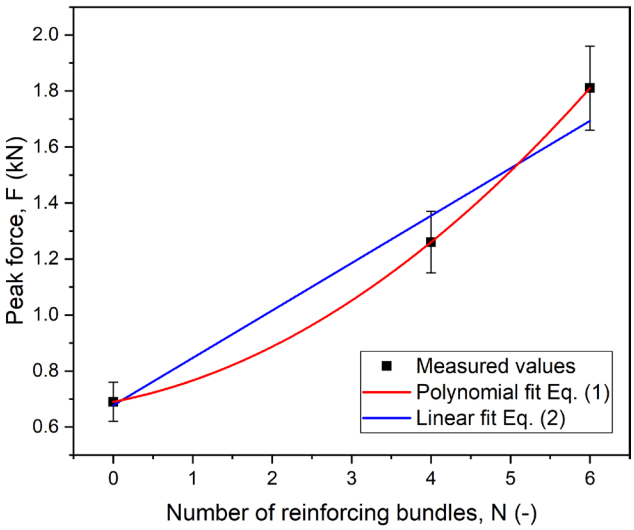

Fig. 9 Relationship between the load-bearing capacity and the number of reinforcing fibre bundles

The characteristic failure behaviour of the specimens is shown in Fig. 10. It can be seen that both specimen types produced the characteristic 45° shear crack. While the placement of the crack varied greatly in the case of the reinforced samples, it was quite uniform in the case of the unreinforced reference samples. In that latter case, the fracture was close to the middle of the specimens.

Last, but not least, the fracture surface was investigated under SEM and a representative example is shown in Fig. 11. The SEM image shows the brittle fracture surface of the expanded glass filler particles and proves the ductile behaviour of the Al99.5 matrix. The reinforcing bundle remained intact in the crack surface and pull-out can be observed from the upper (counterpart – not shown) of the sample.

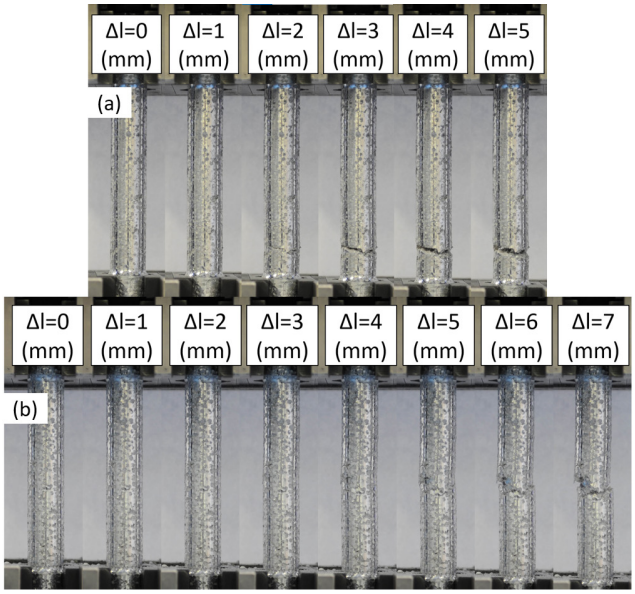

Fig. 10 Characteristic tensile behaviour of the (a) reinforced (4 bundles) and (b) the reference specimens

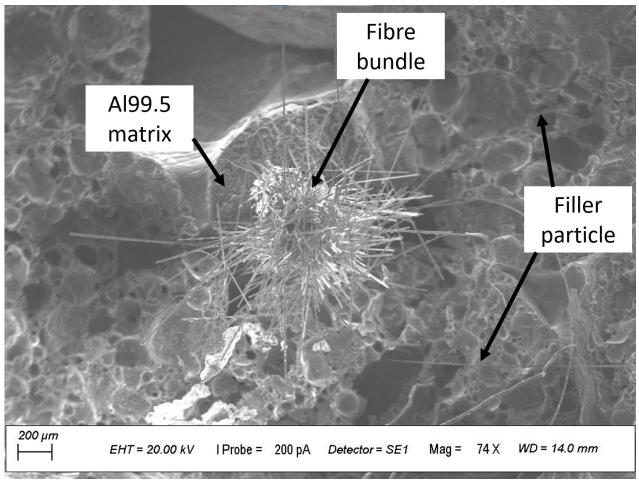

Fig. 11 Fracture surface of a reinforced MMSF in the vicinity of a single reinforcing bundle

4 Conclusions

In this study, the effect of longitudinal partially infiltrated carbon fibre bundle reinforcement on the tensile behaviour of syntactic metal forms was investigated.

The following conclusions were drawn from the experiments:

- Low-pressure infiltration (0.5 MPa) is a suitable method for the production of longitudinally reinforced syntactic metal foams.
- The reinforcement increases the density of the metal foam by 20%, while increasing the tensile load-bearing capacity to ~260% and ~180% in the case of 4 and 6 reinforcing carbon fibre bundles, respectively.
- The relationship between the load-bearing capacity (peak force) and the number of reinforcing carbon fibre bundles can be exactly described by a second-order polynomial function and can also be estimated by a simpler linear relationship.
- Only minimal diffusion of alloying elements occurred between the matrix material and the coating material of the fibre bundles.
- The fibres are easily torn out of the uninfiltrated regions of the bundle. This indicates that only the fully infiltrated parts of the bundle handle the load.
- Both specimen types have a brittle behaviour, which can be attributed to the inner cellular structure.

Acknowledgement

Benedek Szovák was supported by the EKÖP-24-3-BME-4 University Researcher Scholarship Program of the Ministry for Culture and Innovation from the source of the National Research, Development and Innovation Fund.

This work was supported by the National Research, Development and Innovation Office (NKFIH), under grant agreement OTKA-FK_21 138505. Project no. TKP-6-6/PALY-2021 has been implemented with the support provided by the Ministry of Culture and Innovation of Hungary from the National Research, Development and Innovation Fund, financed under the TKP2021-NVA funding scheme.

References

[1] Banhart, J. "Light-Metal Foams - History of Innovation and Technological Challenges", Advanced Engineering Materials, 15(3), pp. 82–111, 2013. https://doi.org/10.1002/adem.201200217

[2] Hannemann, C., Uhlig, M., Hipke, T., Meier, I. "The Challenge of Open Cellular Metal Foam Production", In: Dukhan, N. (ed.) Proceedings of the 11th International Conference on Porous Metals and Metallic Foams (MetFoam 2019), Springer Cham, 2020, pp. 149–157. ISBN 978-3-030-42798-6 https://doi.org/10.1007/978-3-030-42798-6_14

[3] Yu, S., Liu, J., Wei, M., Luo, Y., Zhu, X., Liu, Y. "Compressive property and energy absorption characteristic of open-cell ZA22 foams", Materials & Design, 30(1), pp. 87–90, 2009. https://doi.org/10.1016/j.matdes.2008.04.041

[4] San Marchi, C., Mortensen, A. "Deformation of open-cell aluminum foam", Acta Materialia, 49(19), pp. 3959–3969, 2001. https://doi.org/10.1016/S1359-6454(01)00294-4

[5] Johnson, Q. C., Kenesei, P., Petruzza, S., Plumb, J., Sharma, H., Park, J. S., Marsden, E., Matheson, K., Czabaj, M. W., Spear, A. D. "Mapping 3D grain and precipitate structure during in situ mechanical testing of open-cell metal foam using micro-computed tomography and high-energy X-ray diffraction microscopy", Materials Characterization, 195, 112477, 2023. https://doi.org/10.1016/j.matchar.2022.112477

[6] Linul, E., Galatanu, S.-V., Marsavina, L., Kováčik, J. "Crushing behavior of closed-cell metallic foams: Anisotropy and temperature effects", Journal of Materials Research and Technology, 30, pp. 1436–1449, 2024. https://doi.org/10.1016/j.jmrt.2024.03.186

[7] Naeem, M. A., Gábora, A., Mankovits, T. "Influence of the Manufacturing Parameters on the Compressive Properties of Closed Cell Aluminum Foams", Periodica Polytechnica Mechanical Engineering, 64(2), pp. 172–178, 2020. https://doi.org/10.3311/PPME.16195

[8] Hangai, Y., Ando, M., Ohashi, M., Amagai, K., Suzuki, R., Matsubara, M., Yoshikawa, N. "Compressive properties of two-layered aluminum foams with closed-cell and open-cell structures", Materials Today Communications, 24, 101249, 2020. https://doi.org/10.1016/j.mtcomm.2020.101249

[9] Xia, X. C., Chen, X. W., Zhang, Z., Chen, X., Zhao, W. M., Liao, B., Hur, B. "Effects of porosity and pore size on the compressive properties of closed-cell Mg alloy foam", Journal of Magnesium and Alloys, 1(4), pp. 330–335, 2013. https://doi.org/10.1016/j.jma.2013.11.006

[10] Galațanu, S. V., Marşavina, L., Kováčik, J., Linul, E. "Influence of density and loading speed on static and impact properties of closed-cell metallic foams", Engineering Failure Analysis, 161, 108297, 2024. https://doi.org/10.1016/j.engfailanal.2024.108297

[11] Kincses, D. B., Károly, D., Bukor, C. "Production and testing of syntactic metal foams with graded filler volume", Materials Today: Proceedings, 45, pp. 4225–4228, 2020. https://doi.org/10.1016/j.matpr.2020.12.163

[12] Kádár, C., Kubelka, P., Szlancsik, A. "On the compressive properties of aluminum and magnesium syntactic foams: Experiment and simulation", Materials Today: Communications, 35, 106060, 2023. https://doi.org/10.1016/j.mtcomm.2023.106060

[13] Movahedi, N., Murch, G. E., Belova, I. V., Fiedler, T. "Manufacturing and compressive properties of sandwich foam tubes containing metal syntactic foam", Composite Structures, 316, 117012, 2023. https://doi.org/10.1016/j.compstruct.2023.117012

[14] Taherishargh, M., Vesenjak, M., Belova, I. V., Krstulović-Opara, L., Murch, G. E., Fiedler, T. "In situ manufacturing and mechanical properties of syntactic foam filled tubes", Materials & Design, 99, pp. 356–368, 2016. https://doi.org/10.1016/j.matdes.2016.03.077

[15] Marx, J., Rabiei, A. "Study on the Mechanical Properties of Composite Metal Foam Core Sandwich Panels", In: Dukhan, N. (ed.) Proceedings of the 11th International Conference on Porous Metals and Metallic Foams (MetFoam 2019), Springer Cham, 2020, pp. 83–91. ISBN 978-3-030-42798-6 https://doi.org/10.1007/978-3-030-42798-6_8

[16] Marx, J., Rabiei, A. "Overview of Composite Metal Foams and Their Properties and Performance", Advanced Engineering Materials, 19(11), 1600776, 2017. https://doi.org/10.1002/adem.201600776

[17] Mei, Y., Fu, C., Fu, Y., Ding, Y., Wang, E., Yang, Q. "Tensile Behavior and Performance of Syntactic Steel Foams Prepared by Infiltration Casting", Metals, 12(4), 668, 2022. https://doi.org/10.3390/met12040668

[18] ISO "ISO 21347:2005 - Space systems – Fracture and damage control", International Organization for Standardization, Geneva, Switzerland, 2005.

[19] Thodsaratpreeyakul, W., Uawongsuwan, P., Kataoka, A., Negoro, T., Hamada, H. "The Determination of Interfacial Shear Strength in Short Fiber Reinforced Poly Ethylene Terephthalate by Kelly-Tyson Theory", Open Journal of Composite Materials, 7(4), pp. 218–226, 2017. https://doi.org/10.4236/ojcm.2017.74015

[20] Erannagari, S., Reddy, D. M. "An Experimental Investigation of Natural-fibre/Rubber Reinforced Bio-composites under Low-velocity Impact Analysis", Periodica Polytechnica Mechanical Engineering, 69(2), pp. 129–135, 2025. https://doi.org/10.3311/PPme.39914

[21] Messaoud, B., Amrane, M. N. "Vibration Analysis of Damaged Viscoelastic Composite Sandwich Plate", Periodica Polytechnica Mechanical Engineering, 68(2), pp. 85–96, 2024. https://doi.org/10.3311/ppme.19466

[22] Trivedi, D. N., Munezero, F., Rachchh, N. "Mechanical Characterization of Hybrid Bagasse/Eggshell/E-glass Fiber-based Polyester Composite", Periodica Polytechnica Mechanical Engineering, 68(2), pp. 130–140, 2024. https://doi.org/10.3311/PPme.22963

[23] Máté, P., Szekrényes, A. "The Effect of the Layup on the Stability of Composite Cylindrical Shells", Periodica Polytechnica Mechanical Engineering, 68(4), pp. 291–303, 2024. https://doi.org/10.3311/PPme.23424

[24] Kun, K., Bata, A., Ronkay, F. "Investigation of the Replication Quality of Microstructures on Injection Moulded Specimens Made from Recycled Polypropylene Composites Reinforced with Carbon Nanotubes", Periodica Polytechnica Mechanical Engineering, 68(3), pp. 247–253, 2024. https://doi.org/10.3311/PPme.37288

[25] Kumar, N., Chittappa, H. C., Ezhil Vannan, S. "Development of Aluminium-Nickel Coated Short Carbon Fiber Metal Matrix Composites", Materials Today: Proceedings, 5(5), pp. 11336–11345, 2018. https://doi.org/10.1016/j.matpr.2018.02.100

[26] Vijayaram, T. R., Sulaiman, S., Hamouda, A. M. S., Ahmad, M. H. M. "Fabrication of fiber reinforced metal matrix composites by squeeze casting technology", Journal of Materials Processing Technology, 178(1–3), pp. 34–38, 2006. https://doi.org/10.1016/j.jmatprotec.2005.09.026

[27] Yang, Q., Liu, J., Li, S., Wang, F., Wu, T. "Fabrication and mechanical properties of Cu-coatedwoven carbon fibers reinforced aluminum alloy composite", Materials & Design, 57, pp. 442–448, 2014. https://doi.org/10.1016/j.matdes.2013.12.064

[28] Mileiko, S. "Carbon-Fibre/Metal-Matrix Composites: A Review", Journal of Composites Science, 6(10), 297, 2022. https://doi.org/10.3390/jcs6100297

[29] Ucsnik, S., Großalber, A., Reiter, J., Scheerer, M., Mozdzen, G. "Advances in continuous carbon fibre reinforced Aluminium matrix composites", In: 8th European Conference for Aeronautics and Space Science (EUCASS 2019), Madrid, Spain, 2019, pp. 1–8. https://doi.org/10.13009/EUCASS2019-783

[30] Khanna, V., Kumar, V., Bansal, S. A. "Aluminium-Carbon Fibre Metal Matrix Composites: A Review", IOP Conference Series: Materials Science and Engineering, 1033, 012057, 2021. https://doi.org/10.1088/1757-899X/1033/1/012057

[31] Duarte, I., Ferreira, J. M. F. "Composite and Nanocomposite Metal Foams", Materials, 9(2), 79, 2016. https://doi.org/10.3390/ma9020079

[32] Kientzl, I., Orbulov, I. "Fémmátrixú kompozithuzalok, dupla kompozitok és kompozit tömbök tulajdonságai" (Properties of metal matrix composite wires, double composites, and composite blocks), Anyagok Világa, 7(1), pp. 1–9, 2007. (in Hungarian)

[33] Kientzl, I., Németh, Á., Dobránszky, J. "Influence of the infiltration pressure on the properties of MMC wires", Periodica Polytechnica Mechanical Engineering, 52(1), pp. 15–18, 2008. https://doi.org/10.3311/pp.me.2008-1.03

[34] Kientzl, I., Orbulov, I. N., Dobránszky, J., Németh, Á. "Mechanical Behaviour Al-Matrix Composite Wires in Double Composite Structures", Advances in Science and Technology, 50, pp. 147–152, 2006. https://doi.org/10.4028/www.scientific.net/ast.50.147

[35] Kientzl, I., Dobránszky, J., Németh, Á. "Effect of the infiltration pressure on the properties of composite wires", Materials Science Forum, 659, pp. 177–182, 2010. https://doi.org/10.4028/www.scientific.net/MSF.659.177

[36] ISO "ISO 6892-1:2019 Metallic materials-Tensile testing-Part 1: Method of test at room temperature", International Organization for Standardization, Geneva, Switzerland, 2019.